Spectroscopic Studies of Europium(III) and Gadolinium(III) Tris-β-diketonate Complexes with Diazabutadiene Ligands

José A. Fernandes,[a] Rute A. Sá Ferreira,[b] Martyn Pillinger,[a] Luís D. Carlos,*[b] Isabel S. Gonçalves,[a] and Paulo J. A. Ribeiro-Claro*[a]

Keywords: Ab initio calculations / Lanthanides / Luminescence / N ligands / Vibrational spectroscopy

Adducts of the type $Ln(NTA)_3$·L [Ln = Eu, Gd; NTA = 1-(2-naphthoyl)-3,3,3-trifluoroacetonate; L = 1,4-diaza-1,3-butadiene RN=CHCH=NR (R = *p*-tolyl, *o*-tolyl)] were prepared by treatment of $Ln(NTA)_3·2H_2O$ with one equivalent of the chelating N–N ligand. The mixed ligand complexes were characterised by elemental analysis, thermogravimetric analysis, IR and Raman spectroscopy, and photoluminescence (PL) spectroscopy. Ab initio calculations were carried out in order to predict coordination geometries and also to interpret the vibrational spectra. For the europium(III) compounds, new Raman-active bands at approximately 440 and 479 cm^{-1} are tentatively assigned to $(\nu Eu–N)_{sym}$ and $(\nu Eu–N)_{as}$ modes, respectively. A second band at 1185 cm^{-1} is associated with the symmetric stretching of the N–C(ring) and C–C (DAB) bonds, and is shifted about 20 cm^{-1} to a higher wavenumber relative to the corresponding band for the free ligand. The room-temperature PL spectra of the two Eu complexes are composed of the typical Eu^{3+} red emission, assigned to transitions between the first excited state ($^5D_0$) and the ground multiplet ($^7F_{0–4}$). Based on the room-temperature emission spectra and lifetime measurements, the quantum efficiencies of the $^5D_0$ Eu^{3+} excited state were estimated and found to be quite low (e.g. 2–3%). The low efficiencies are attributed to the presence of thermally activated nonradiative channels involving ligand-to-metal charge-transfer (LMCT) states. Indeed, a low-lying LMCT band was detected for the Eu complex containing the ligand *p*-tolyl-DAB by comparison of the room-temperature diffuse reflectance spectrum for this complex with that of the corresponding Gd analogue.

Introduction

Over the past 40 years there has been considerable interest in the luminescence and lasing ability of certain diketonates of lanthanides, particularly europium(III) and terbium(III).[1–4] Two classes of complexes may be distinguished depending on whether the ratio of diketonate ion to metal ion in the product is 3:1 (tris complex) or 4:1 (tetrakis complex).[5,6] The tris-β-diketonates are usually coordinatively unsaturated and, therefore, form adducts with a variety of Lewis base ligands, to give seven-, eight- or even nine-coordinate complexes.[7–19] Some of us recently reported on the luminescence features and the absolute quantum yield of europium(III) tris[1-(2-naphthoyl)-3,3,3-trifluoroacetonate] complexes, $Eu(NTA)_3·2L$ (NTA = 1-(2-naphthoyl)-3,3,3-trifluoroacetonate, L = H_2O and DMSO).[19] The experimental quantum yield measured for $Eu(NTA)_3·2DMSO$ (0.75) is one of the highest so far reported for solid-state europium complexes. Replacement of the solvent molecules in these complexes by organic ligands is one way to further modify the luminescence properties of the parent tris complex. The complex with 2,2′-bipyridine (bipy) has already been reported.[9] In the present work, $Eu(NTA)_3$ complexes containing 1,4-diaza-1,3-butadienes (DAB) of the type RN=CR′CR′=NR (R = *p*-tolyl, *o*-tolyl; R′ = H) have been prepared and characterised. For comparison, the corresponding Gd^{III} complexes have also been prepared. To the best of our knowledge, very few studies have been carried out on diazabutadiene compounds of rare earths,[20–22] especially with regard to their photophysical properties. This is surprising since, as α-diimine ligands, DAB ligands have electronic and structural similarities to the more extensively studied heteroaromatic chelating agents bipy and 1,10-phenanthroline.[23] Added flexibility arises from the presence of the substituents R and R′, perhaps allowing luminescence behaviour to be tuned by variation of steric and electronic effects.

Results and Discussion

Synthesis and Thermogravimetric Analysis

The mononuclear complexes $Ln(NTA)_3$·*p*-tolyl−DAB [Ln = Eu (**1**), Gd (**3**)] and $Ln(NTA)_3$·*o*-tolyl−DAB [Ln =

[a] Department of Chemistry, CICECO, University of Aveiro, 3810-193 Aveiro, Portugal
Fax: (internat.) + 351-234-370084
E-mail: pclaro@dq.ua.pt
[b] Department of Physics, CICECO, University of Aveiro, 3810-193 Aveiro, Portugal

Eu (**2**), Gd (**4**)] were prepared in reasonable yields by the treatment of solutions of $Ln(NTA)_3{\cdot}2H_2O$ in chloroform with one equivalent of the respective diazabutadiene ligand.

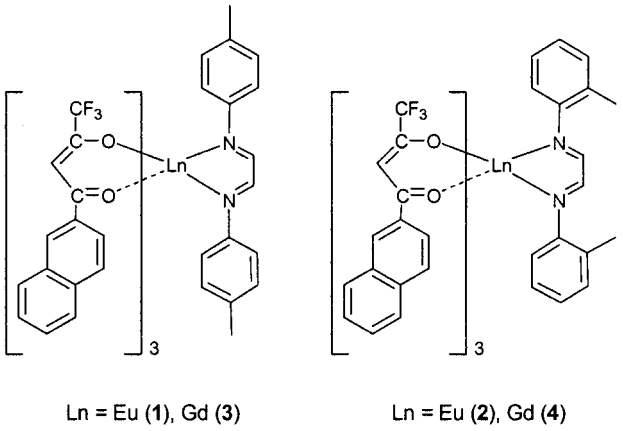

Figure 1 shows the TGA results for *o*-tolyl−DAB, $Eu(NTA)_3{\cdot}2H_2O$ and $Eu(NTA)_3{\cdot}$*o*-tolyl−DAB (**2**). Similar traces were obtained for the compounds *p*-tolyl−DAB, $Gd(NTA)_3{\cdot}2H_2O$ and $Ln(NTA)_3{\cdot}$L (**1**,**3**,**4**), respectively. The compounds *o*-tolyl−DAB and *p*-tolyl−DAB sublime in the temperature range 100−230 °C. The precursors $Ln(NTA)_3{\cdot}2H_2O$ undergo a mass loss up to 100 °C, which corresponds to the removal of coordinated water. Further decomposition takes place in two steps; the first of these occurs between 100 and 350 °C (54% mass loss for Eu, 63% for Gd), and the second between 350 and 600 °C (21% mass loss for Eu, 19% for Gd). Finally, a small mass loss of 2% occurs between 600 and 700 °C for both compounds, leaving a residual mass of 17.7% for Eu and 13.8% for Gd. The TGA curves of the adducts **1**−**4** are very similar to each other and to the reagents $Ln(NTA)_3{\cdot}2H_2O$, and all steps for these six compounds take place at the same temperatures. There is no step characteristic of "free" ligand, indicating that the ligands are coordinated to the metal centres. The first mass loss (3.0% for **1**) corresponds to the removal of water content. Following this, the mass loss for the step between 100 and 350 °C is smaller than that observed for the reagents (47.2% for compound **1**). Conversely, the step between 350 and 600 °C corresponds to a larger amount (34.3% for compound **1**). Finally, the TGA shows a mass loss of about 2% between 575 and 720 °C, leaving a residual mass of about 16% for compounds **1** and **2**, and 14% for compounds **3** and **4**.

Ab Initio Calculations and Vibrational Spectra

Figure 2 shows the calculated coordination geometry of DAB in **1** (NTA ligands are shown in wireframe). The complexed tolyl−DAB adopts a propeller-like configuration; the phenyl rings are rotated 33° and 42° from the N=C−C=N plane, in opposite directions. In the free ligand, the lowest energy form presents a similar rotation angle (approximately 37°), but to the same side of the N=C−C=N plane (therefore, the phenyl rings are co-planar). Similar results were obtained for the simulation of *o*-tolyl−DAB

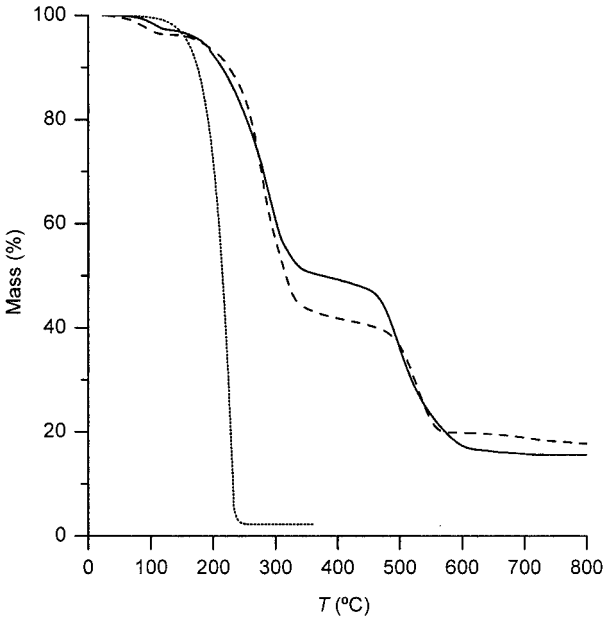

Figure 1. TGA of $Eu(NTA)_3{\cdot}$*o*-tolyl−DAB (**2**) (−), *o*-tolyl−DAB (···) and $Eu(NTA)_3{\cdot}2H_2O$ (− − −)

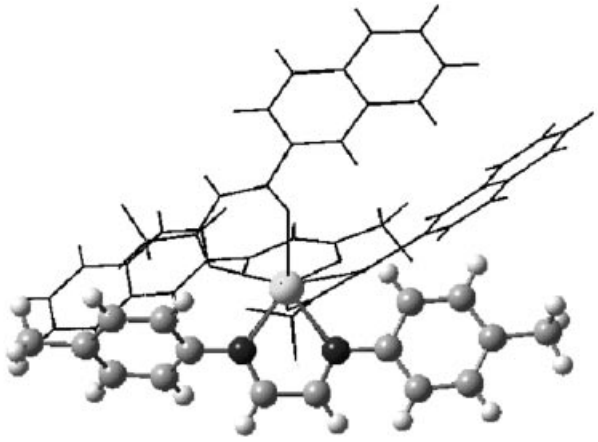

Figure 2. Lowest energy structure calculated for the model $Eu[O(CH)_3O]_3{\cdot}$*p*-tolyl−DAB; the $(NTA)_3$ framework was obtained from the X-ray single crystal structure for $Eu(NTA)_3{\cdot}$phenanthroline[24]

(**2**), with the exception of the twist angles of the phenyl ring, which are about 10° larger than those for **1** due to the presence of the *ortho* methyl groups. Calculated Eu−N distances are about 233 pm, and the N−Eu−N angle is 72° in both **1** and **2**. The Eu−N bond lengths are shorter than those calculated at the same level for the 2,2′-bipyrimidine and 1,10-phenanthroline derivatives,[24] suggesting a stronger Eu−N interaction in the case of the present ligands. As a result, the calculated frequencies for the Eu−N stretching modes are higher than those usually reported. In fact, ab initio calculations predict the νEu−N stretching modes at about 460 cm^{-1} (after scaling), with a moderately strong Raman intensity and weak IR intensity.

An important geometrical change upon complexation is revealed in the bond lengths of the diazabutadiene fragment. From the free DAB ligand to complex **1**, the

$C_{(ring)}-N$, C=N and C−C bond lengths are reduced by approximately 2.2, 1.8 and 3.3 pm, respectively. From the free ligand to complex **2**, the corresponding values are 1.7, 1.8 and 2.9 pm, respectively. The effect is residual in the aromatic C−C bonds (< 1 pm) and is absent in the $C-CH_3$ bonds. This contraction affects the vibrational modes involving the diazabutadiene fragment, which are predicted to be generally shifted to higher wavenumbers upon complexation. The effect is particularly evident in the mode combining the symmetric stretching of the $N-C_{(ring)}$ and C−C (DAB) bonds, with a strong Raman intensity, for which a shift of 20 cm^{-1} is predicted. The calculated scaled values are 1164 cm^{-1} for the free DAB ligands and 1184 cm^{-1} for the complex model. These predictions find experimental support from the vibrational spectra, as discussed below.

The vibrational spectra of **1** and **2** are well-described by the sum of the spectra of their reagents, with some additional details ascribed to the complexation process. Figure 3 shows two relevant regions in the Raman spectra of compound **1** [trace (c)], the reagents $Eu(NTA)_3{\cdot}2H_2O$ [trace (b)] and *p*-tolyl−DAB [trace (a)].

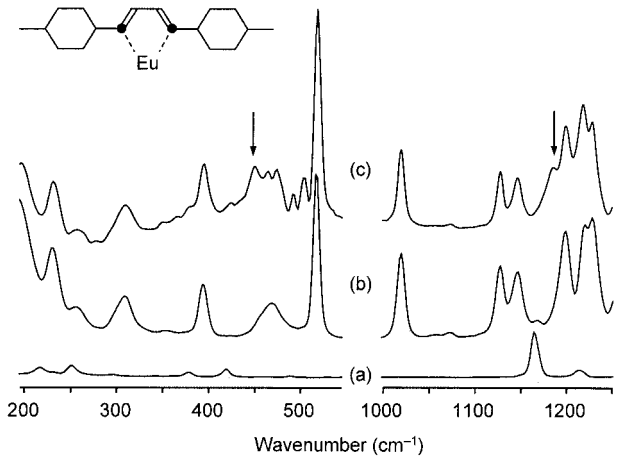

Figure 3. Raman spectra of (a) *p*-tolyl−DAB, (b) $Eu(NTA)_3{\cdot}2H_2O$ and (c) $Eu(NTA)_3$·*p*-tolyl−DAB (**1**); the arrows point to the bands assigned to the *ν*Eu−N modes (about 460 cm^{-1}) and symmetric stretching of the N−C(ring) and C−C (DAB) bonds (1185 cm^{-1})

The vibrational modes involving the Eu−N bonds were searched for in the low wavenumber region. The two bands observed at approximately 440 and 479 cm^{-1} are not present in the spectra of the reagents and fit the intensity and wavenumber predicted from ab initio calculations. In this way, they have been tentatively assigned to $(\nu Eu-N)_{sym}$ and $(\nu Eu-N)_{as}$, respectively. Identical bands are observed at 449 cm^{-1} and 473 cm^{-1} in the Raman spectrum of **2**, supporting this assignment. Analysis of the IR spectrum in this region was inconclusive, due to band overlap.

The effect of complexation can also be observed in the higher wavenumber region of Figure 3. The bands corresponding to the symmetric stretching of the $N-C_{(ring)}$ and C−C (DAB) bonds are easily identified in the spectra of the free ligands and products due to their strong Raman intensity. As can be seen, the strong band at 1165 cm^{-1} for the pure DAB ligand [trace (a)] moves to about 1185 cm^{-1} in **1** [trace (c)]. The ca. 20 cm^{-1} upwards shift upon complexation is in agreement with the contraction of the C−C and N−C bonds from the free ligand to the complexes.

Photoluminescence Studies

Figure 4 shows the room-temperature PL spectra of compounds **1** and **2** obtained under the excitation wavelength that maximises the emission intensity. Both spectra are composed of the typical Eu^{3+} red emission, assigned to transitions between the first excited state ($^5D_0$) and the ground multiplet ($^7F_{0-4}$). It is possible to identify 3 and 5 Stark components for the $^5D_0 \rightarrow {}^7F_{1-2}$ transitions, which indicates that the Eu^{3+} ions are located in a low site symmetry group, without an inversion centre according to the higher intensity of the $^5D_0 \rightarrow {}^7F_2$ transition. Changes in the excitation wavelength did not produce significant alterations either in the number of emission components or in their energy. The presence of only one component for the $^5D_0 \rightarrow {}^7F_0$ transition suggests only one Eu^{3+} local environment. However, the high value found for the full width at half maximum (fwhm) in both compounds(26 cm^{-1}) indicates a large distribution of local coordination sites,[25] probably induced by the amorphous nature of the compounds. The similarity between the two spectra is also apparent in the energy and fwhm of the $^5D_0 \rightarrow {}^7F_{0-2}$ transitions. This fact, in particular the comparable energies for the $^5D_0 \rightarrow {}^7F_0$ transition, indicates that the Eu^{3+} first coordination sphere might be very similar for the two compounds. This is based on the knowledge that the energy of this transition is usually related to the so-called *nephelauxetic* effect induced by the ion′s first neighbours.[26] Such conclusions are also supported by the PL spectra measured at 14 K. Apart from small changes in the relative intensity of the $^5D_0 \rightarrow {}^7F_2$ transition Stark components, the energy, fwhm and number of emission components of the intra-$4f^6$ transitions are essentially the same as observed at room

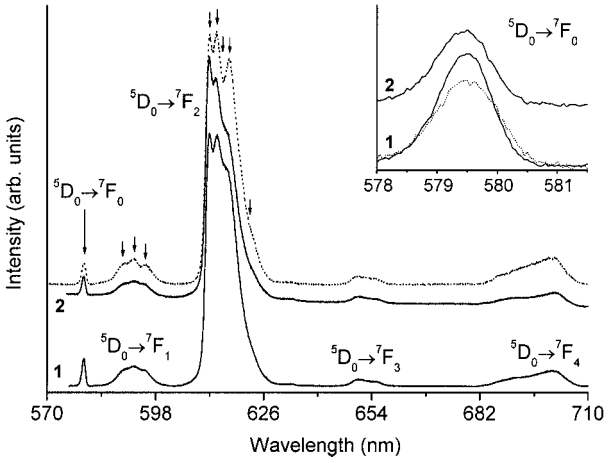

Figure 4. Room-temperature PL spectra of compounds **1** and **2** excited at 345 nm; The dotted line corresponds to the PL spectrum of **1** detected at 14 K and excited at 365 nm

temperature. However, the integrated intensity of the emission arising from the $^5D_0$ level strongly depends on the selected temperature, presenting the behaviour shown in Figure 5 for **1**. For both compounds, no emission from the ligands could be detected, suggesting an effective interaction between them and the Eu^{3+} ions.

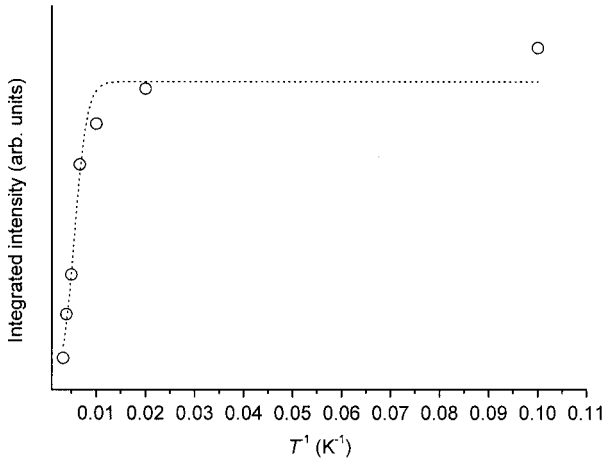

Figure 5. Temperature-dependence (14−300 K) of the Eu^{3+} $^5D_0$ emission for compound **1** (open circles); the dotted line is the best fit to the data using Equation (4)

The excitation spectra (PLE), monitored around the most intense line of the cation (Figure 6), enable us to draw the same conclusion. The spectra exhibit a large broad band between 280 and 420 nm, with a maximum at around 345 nm, and no lines associated with the direct excitation of the intra-$4f^6$ levels are detected. This strongly suggests an efficient sensitization process between the ligands and the metal ion. Lowering the temperature to 14 K induces a red-shift to 365 nm, and a low-intensity line associated with the excitation of the $^5D_2$ level is observed, as shown in Figure 6 for **1**. This large band may originate from the ligand levels involving the NTA and diimine components, since the PLE spectrum acquired for $Eu(NTA)_3{\cdot}2H_2O$ under identical experimental conditions is different from those plotted in Figure 6.[19]

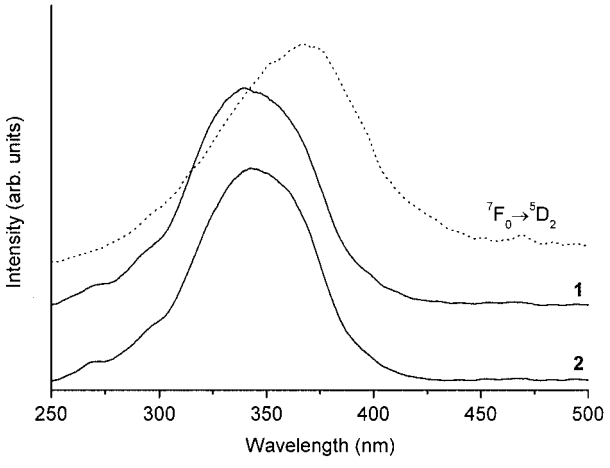

Figure 6. room-temperature PLE spectra of compounds **1** and **2** monitored around 612 nm; the dotted line is the PLE spectrum of **1** detected at 14 K

The $^5D_0$ lifetime, τ, was measured around the most intense PL line (not shown). For both compounds the data are well described by a single exponential function, revealing lifetime values of 0.038 ± 0.001 and 0.030 ± 0.001 ms for compounds **1** and **2**, respectively. These values are smaller than the lifetime value previously found for the precursor complex.[19]

Based on the room-temperature emission spectra and on the lifetime measurements we can estimate the efficiency, q, of the $^5D_0$ Eu^{3+} excited state, considering that only nonradiative and radiative processes are essentially involved in the depopulation of the $^5D_0$ state,[3,19,27,28] where k_r and k_{nr} are the radiative and nonradiative transition probabilities, respectively, ($k_{exp} = 1/\tau_{exp} = k_r + k_{nr}$).

$$q = \frac{k_r}{k_r + k_{nr}} \tag{1}$$

The emission intensity, I, taken as the integrated intensity, S, of the emission curves, for the $^5D_0 \rightarrow {}^7F_{0-4}$ transitions, is expressed by Equation (2): where i and j represent the initial ($^5D_0$) and final ($^7F_{0-6}$) levels, respectively, $\hbar w_{i\rightarrow j}$ is the transition energy, $A_{i\rightarrow j}$ corresponds to Einstein's coefficient of spontaneous emission and N_i is the population of the $^5D_0$ emitting level.[3,19,27,28]

$$I_{i\rightarrow j} = \hbar w_{i\rightarrow j} A_{i\rightarrow j} N_i \equiv S_{i\rightarrow j} \tag{2}$$

The radiative contribution may be calculated from the relative intensities of the $^5D_0 \rightarrow {}^7F_{0-6}$ transitions. Since the $^5D_0 \rightarrow {}^7F_1$ transition can be considered as a reference due to its dipolar magnetic nature, k_r can be calculated according to Equation (3), where $A_{0\rightarrow 1}$ is the Einstein's coefficient of spontaneous emission between the $^5D_0$ and the $^7F_1$ Stark levels.

$$k_r = A_{0\rightarrow 1} \frac{\hbar\omega_{0\rightarrow 1}}{S_{0\rightarrow 1}} \sum_{J=0}^{6} \frac{S_{0-J}}{\hbar\omega_{0-J}} \tag{3}$$

The $^5D_0 \rightarrow {}^7F_{5,6}$ transitions were not measured experimentally and so the branching ratio for these transitions, which is usually very small, can be neglected. Therefore, we can ignore their influence in the depopulation of the $^5D_0$ excited state. The $^5D_0 \rightarrow {}^7F_1$ transition does not depend on the local ligand field seen by Eu^{3+} ions and, thus, may be used as a reference for the whole spectrum; in vacuo $A(^5D_0 \rightarrow {}^7F_1) = 14.65\ s^{-1}$.[28] The values found for q, k_r and k_{nr} for compounds **1** and **2** are gathered in Table 1. An average index of refraction equal to 1.5 was considered for both compounds leading to an approximate $A(^5D_0 \rightarrow {}^7F_1)$ value of $50\ s^{-1}$.[29]

Table 1. Experimental $^5D_0$ lifetimes (τ) and decay rates (k_{exp}), calculated radiative (k_r) and nonradiative (k_{nr}) $^5D_0$ decay rates and quantum efficiency (q) for compounds **1** and **2**

	τ (ms)	k_{exp} (ms^{-1})	k_r (ms^{-1})	k_{nr} (ms^{-1})	q (%)
1	0.038 ± 0.001	26.32	0.82	25.50	3.1
2	0.030 ± 0.001	33.33	0.72	32.61	2.2

Compound **1** has the highest q value, induced by higher k_r (12%) and lower k_{nr} (22%) values. However, both compounds present lower values for the $^5D_0$ quantum efficiency compared with that found for the precursor complex $Eu(NTA)_3{\cdot}2H_2O$ (q = 29%)[19] that may be induced by the higher k_{nr} contribution found in **1** and **2**. In fact, the temperature-dependence of the Eu^{3+} emission-integrated intensity, I_{int} (Figure 5), suggests a thermally activated nonradiative mechanism. Such nonradiative de-excitation is well-described by the following expression:

$$I_{int} = \frac{1}{1 + A\exp(-E_a/K_BT)} \quad (4)$$

where A is related to the ratio between the nonradiative (at $T = 0$) and radiative rates, K_B is the Boltzmann constant and E_a is the energy of activation of the de-excitation channel with respect to the energy of the $^5D_0$ level. The energy activation obtained is 550 ± 136 cm^{-1}, which places the nonradiative level in a position resonant with the Eu^{3+} emitting level.

In Eu^{3+} complexes such thermally activated nonradiative channels may involve ligand-to-metal charge-transfer (LMCT) states, formed by the orbital overlap of the ligand and Eu^{3+} energy levels.[30−32] Quenching of the Eu^{3+} PL by low-lying thermally activated LMCT transitions is a well-known phenomenon in molecular solids and complexes in solution.[31−34] These states are usually difficult to detect by absorption and emission spectroscopy, and indeed their unequivocal assignment and detection have only been performed for a few lanthanide compounds.[3,31−34] Due to the difficulties in detecting LMCT states, they are usually claimed to exist in order to explain low PL quantum yields and/or the strong dependence of the emission intensity with temperature. The comparison of Eu^{3+} and Gd^{3+} reflectance spectra is a useful tool to perceive and ascribe the LMCT transitions, since the energetic difference between the Gd^{3+} first excited state and the fundamental levels is too high to allow the detection of a charge-transfer state in the UV/Vis range. Therefore, in the Gd^{3+} spectrum we expect to measure only the contributions that are not related with the LMCT processes.

Figure 7 shows the room-temperature diffuse reflectance spectra of compounds **1** and **3**. The arithmetic difference between the two curves is also represented, showing the presence of a low-lying LMCT band (centred at about 17800 cm^{-1}). As far as we know, this is one of the clearest examples where the arithmetic difference between the diffuse reflectance spectra of isostructural Eu^{3+} and Gd^{3+} compounds allows the explicit identification of ligand-to-metal charge transfer states by direct means. Unfortunately, and in agreement with the mentioned difficulties, these states cannot be identified so visibly in the reflectance spectra of compounds **2** and **4**.

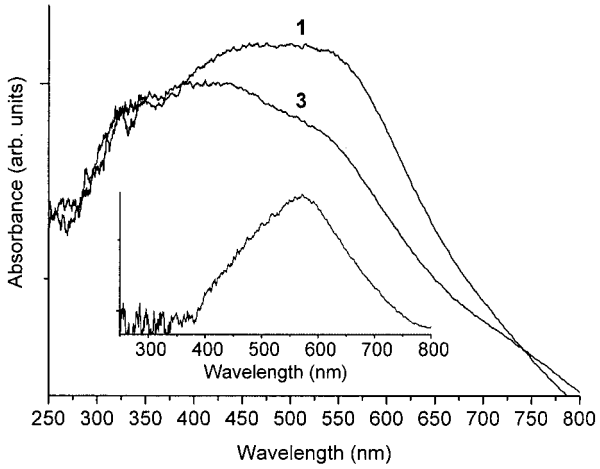

Figure 7. room-temperature diffuse reflectance spectra of compounds **1** and **3**; the arithmetic difference between the two curves is also represented

The charge-transfer band observed in the reflectance spectrum of compound **1** (Figure 7) does not appear at all as an excitation band (see the PLE spectra of Figure 6), indicating that the LMCT band in these compounds is predominantly a quenching channel. This is exactly the conclusion arrived at previously from the temperature-dependence of the Eu^{3+} emission integrated intensity of compound **1** (Figure 5). Actually, the energy of the thermally activated nonradiative level derived from Equation (4), 550 ± 136 cm^{-1} above the $^5D_0$ level (about 17256.3 cm^{-1}, Figure 4), is in excellent agreement with the maximum of the LMCT band discerned from the arithmetic difference between the reflectance spectra of **1** and **3** (approximately 17800 cm^{-1}, Figure 7). Therefore, the low $^5D_0$ quantum efficiency observed for compounds **1** and **2** can be reliably assigned to a nonradiative decay through the LMCT state of Eu^{3+}, which is at rather low energies in these diimine compounds. This is in agreement with previously reported experimental results that indicate that the $^5D_0$ quantum efficiency decreases as the energy of the LMCT states decreases.[31,32] Moreover, recent theoretical results on energy transfer mechanisms between these LMCT states and the ligand and Eu^{3+} levels demonstrate that the quantum yield of the complex (and thus the $^5D_0$ quantum efficiency) decreases drastically as the LMCT barycentre becomes resonant with the $^5D_0$ level.[35]

Concluding Remarks

New europium and gadolinium tris-β-diketonate complexes have been prepared, containing diazabutadiene (DAB) ligands coordinated to the metal centres. Accordingly, the complexes with the general formula $Ln(NTA)_3{\cdot}nL$ (Ln = Eu, Gd) are now known with L = H_2O, DMSO, 2,2′-bipyridine, 1,10-phenanthroline and DAB. Binuclear complexes of the type $[Ln(NTA)_3]_2{\cdot}$bpym (bpym = 2,2′-bipyrimidine) have also been reported. The motivation for the preparation of these derivatives stems from the fact that the experimental quantum yield measured for $Eu(NTA)_3{\cdot}2DMSO$ (0.75) is one of the highest so far reported for solid-state europium complexes. It has been found that the $^5D_0$ quantum efficiencies for these complexes vary considerably depending on the nature of L, decreasing in the order L = DMSO (62%), phen (40%), bpym (39%), H_2O (29%) and DAB (2−3%). The low $^5D_0$ quantum efficiencies for the diazabutadiene adducts can be reliably assigned to a nonradiative decay through the LMCT state of Eu^{3+}, which is at rather low energies in these diimine compounds. The use of photoluminescence spectroscopy, together with vibrational spectroscopy and ab initio calculations, therefore allows us to build up quite a detailed picture about the nature of the metal−ligand interactions in these tris-β-diketonate complexes.

Experimental Section

Materials and Methods: $Eu(NTA)_3{\cdot}2H_2O$,[36] $Gd(NTA)_3{\cdot}2H_2O$,[36] *p*-tolyl−DAB,[37] and *o*-tolyl−DAB[37] were prepared by literature methods.

Microanalyses were performed at the Instituto de Tecnologia Química e Biológica (ITQB), Lisbon. Thermogravimetric analyses (TGA) were performed using a Mettler TA3000 system at a heating rate of 5 K min^{-1} under a static atmosphere of air. IR spectra were obtained as KBr pellets with a FTIR Mattson-7000 infrared spectrophotometer. Raman spectra were recorded with a Bruker RFS100/S FT instrument (Nd:YAG laser, 1064 nm excitation, InGaAs detector). The photoluminescence spectra (PL) were recorded on a Jobin Yvon-Spex spectrometer (HR, 460) coupled to a R928 Hamamatsu photomultiplier (14−300 K). A 300 W Xe arc lamp coupled to a Jobin Yvon-Spex (TRIAX 180) monochromator was used as the excitation source. All the spectra were corrected for the response of the detector. The lifetime measurements were carried out at room temperature (r.t.) on a modular double grating excitation spectrofluorimeter with a TRIAX 320 emission monochromator (Fluorolog-3, Jobin Yvon-Spex) in front face mode coupled to a R928 Hamamatsu photomultiplier.

Preparation of Complexes: A solution of the diimine (0.102 g, 0.432 mmol) in $CHCl_3$ (5 mL) was added to a solution of $Ln(NTA)_3{\cdot}2H_2O$ (0.432 mmol) in $CHCl_3$ (15 mL). The reaction mixture was stirred for 3 h at room temperature. The solvent was then removed, and the resultant brown solid was washed with hexane and dried in vacuo.

$Eu(NTA)_3{\cdot}$*p*-tolyl−DAB (1): Yield: 0.455 g (89%). $C_{58}H_{40}EuF_9N_2O_6$ (1183.9): calcd. C 58.84, H 3.41, N 2.37; found C 58.89, H 3.46, N 2.37. IR (KBr, selected): $\tilde{\nu}_{max.}$ = 3065 (w), 2961 (w), 2927 (w), 1614 (s), 1593 (m), 1570 (m), 1531 (m), 1510 (m), 1460 (m), 1384 (w), 1353 (w), 1298 (s), 1251 (m), 1198 (m), 1135 (m), 1074 (w), 959 (w), 865 (w), 792 (m), 749 (w), 684 (m), 568 (w), 472 (w) cm^{-1}. Raman: 3058 (m), 1629 (s), 1596 (m), 1468 (s), 1432 (w), 1386 (s), 1298 (m), 1228 (w), 1199 (w), 1019 (w), 771 (m), 517 (m) cm^{-1}.

$Eu(NTA)_3{\cdot}$*o*-tolyl−DAB (2): Yield: 0.441 g (82%). $C_{58}H_{40}EuF_9N_2O_6$ (1183.9): calcd. C 58.84, H 3.41, N 2.37; found C 58.78, H 3.33, N 2.28. IR (KBr, selected): $\tilde{\nu}_{max.}$ = 3060 (w), 2959 (w), 2924 (w), 1613 (vs), 1593 (s), 1570 (s), 1532 (s), 1509 (s), 1460 (m), 1384 (w), 1353 (w), 1298 (vs), 1251 (m), 1198 (s), 1136 (s), 1074 (w), 958 (w), 864 (w), 793 (m), 749 (m), 684 (m), 569 (w), 519 (w), 472 (w) cm^{-1}. Raman: 3056 (m), 1628 (s), 1596 (m), 1532 (m), 1468 (s), 1432 (w), 1386 (s), 1297 (m), 1228 (w), 1198 (w), 1019 (w), 771 (m), 517 (m) cm^{-1}.

$Gd(NTA)_3{\cdot}$*p*-tolyl−DAB (3): Yield: 0.255 g (46%). $C_{58}H_{40}F_9GdN_2O_6$ (1189.2): calcd. C 58.58, H 3.39, N 2.36; found C 58.43, H 3.21, N 2.29. IR (KBr, selected): $\tilde{\nu}_{max.}$ = 3058 (w), 2960 (w), 2958 (w), 1615 (s), 1570 (m), 1532 (m), 1510 (m), 1384 (vs), 1299 (m), 1198 (m), 1135 (m), 959 (w), 792 (m), 684 (m), 570 (w), 471(w) cm^{-1}. Raman: 3057 (m), 1629 (s), 1596 (m), 1468 (s), 1432 (w), 1386 (s), 1299 (m), 1228 (w), 1198 (w), 1019 (w), 770 (m), 517 (m) cm^{-1}.

$Gd(NTA)_3{\cdot}$*o*-tolyl−DAB (4): Yield: 0.168 g (39%). $C_{58}H_{40}F_9GdN_2O_6$ (1189.2): calcd. C 58.58, H 3.39, N 2.36; found C 58.75, H 3.33, N 2.38. IR (KBr, selected): $\tilde{\nu}_{max.}$ = 3058 (w), 2960 (w), 2926 (w), 1614 (vs), 1594 (s), 1570 (s), 1531 (s), 1509 (s), 1460 (m), 1384 (m), 1353 (m), 1298 (s), 1251 (m), 1187 (s), 1135 (s), 1074 (w), 958 (w), 865 (w), 792 (m), 748 (m), 684 (m), 568 (w), 472 (w) cm^{-1}. Raman: 3057 (m), 1628 (s), 1596 (m), 1532 (m), 1467 (s), 1432 (w), 1386 (s), 1297 (m), 1227 (w), 1197 (w), 1019 (w), 770 (m), 517 (m) cm^{-1}.

Ab Initio Calculations: Ab initio calculations were performed using the G03w program package,[38] running on a personal computer. The fully optimised geometry, the harmonic vibrational frequencies, and the infrared and Raman intensities were obtained at the B3LYP level, using the Effective Core Potentials (ECP) of Pacios and Christiansen[39] and *f* function (zeta = 0.591) for the Eu atom, and the Stevens/Basch/Krauss[40,41] ECP minimal basis set (CEP-4G option of G03) for the remaining atoms. Due to the large size of the systems, the NTA ligands were replaced by the coordination fragment $[O(CH)_3O]^-$. This model consistently yields Eu−O and Eu−N bond lengths shorter than the reported X-ray values for the phenanthroline,[24] bipyridine,[24] and diaquo[42] analogues, by 16% and 7%, respectively. The calculated wavenumbers were scaled by a factor of 0.90 before comparison with the experimental values.

Acknowledgments

The authors are grateful to FCT, POCTI and FEDER for financial support (Project POCTI/CTM/46780/2002). J. F. thanks the University of Aveiro and the FCT for research grants.

[1] L. C. Thompson, in *Handbook on the Physics and Chemistry of Rare Earths* (Eds.: K. A. Gscheidner, Jr. and L. Eyring), North-Holland, Amsterdam, **1979**, vol. 3, chapter 25.
[2] W. DeW. Horrocks, M. Albin, *Prog. Inorg. Chem.* **1984**, *31*, 1.
[3] G. F. de Sá, O. L. Malta, C. de Mello Donegá, A. M. Simas, R. L. Longo, P. A. Santa-Cruz, E. F. da Silva, *Coord. Chem. Rev.* **2000**, *196*, 165.
[4] K. C. Joshi, V. N. Pathak, *Coord. Chem. Rev.* **1977**, *22*, 37.
[5] L. R. Melby, N. J. Rose, E. Abramson, J. C. Caris, *J. Am. Chem. Soc.* **1964**, *86*, 5117.

[6] H. Bauer, J. Blanc, D. L. Ross, *J. Am. Chem. Soc.* **1964**, *86*, 5125.
[7] A. K. Trikha, L. B. Zinner, K. Zinner, P. C. Isolani, *Polyhedron* **1996**, *15*, 1651.
[8] H. J. Batista, A. V. M. de Andrade, R. L. Longo, A. M. Simas, G. F. de Sá, N. K. Ito, L. C. Thompson, *Inorg. Chem.* **1998**, *37*, 3542.
[9] L. C. Thompson, F. W. Atchison, V. G. Young, *J. Alloys Compd.* **1998**, *275−277*, 765.
[10] K. Iftikhar, M. Sayeed, N. Ahmed, *Inorg. Chem.* **1982**, *21*, 80.
[11] D. F. Moser, L. C. Thompson, V. G. Young Jr., *J. Alloys Compd.* **2000**, *303−304*, 121.
[12] O. L. Malta, M. A. Couto dos Santos, L. C. Thompson, N. K. Ito, *J. Lumin.* **1996**, *69*, 77.
[13] V. Tsaryuk, J. Legendziewicz, L. Puntus, V. Zolin, J. Sokolnicki, *J. Alloys Compd.* **2000**, *300−301*, 464.
[14] R. C. Holz, L. C. Thompson, *Inorg. Chem.* **1993**, *32*, 5251.
[15] L. C. Thompson, S. Berry, *J. Alloys Compd.* **2001**, *323−324*, 177.
[16] R. C. Holz, L. C. Thompson, *Inorg. Chem.* **1988**, *27*, 4640.
[17] O. L. Malta, H. F. Brito, J. F. S. Menezes, F. R. Gonçalves e Silva, C. de Mello Donegá, S. Alves Jr., *Chem. Phys. Lett.* **1998**, *282*, 233.
[18] O. L. Malta, H. F. Brito, J. F. S. Menezes, F. R. Gonçalves e Silva, S. Alves Jr., F. S. Farias Jr., A. V. M. de Andrade, *J. Lumin.* **1997**, *75*, 255.
[19] L. D. Carlos, C. de Mello Donegá, R. Q. Albuquerque, S. Alves Jr., J. F. S. Menezes, O. L. Malta, *Mol. Phys.* **2003**, *101*, 1037.
[20] G. van Koten, K. Vrieze, *Adv. Organomet. Chem.* **1982**, *21*, 151.
[21] F. G. N. Cloke, H. C. Delemos, A. A. Sameh, *J. Chem. Soc., Chem. Commun.* **1986**, 1344.
[22] F. G. N. Cloke, *Chem. Soc. Rev.* **1993**, *22*, 17.
[23] M. N. Bochkarev, A. A. Trifonov, F. G. N. Cloke, C. I. Dalby, P. T. Matsunaga, R. A. Andersen, H. Schumann, J. Loebel, H. Hemling, *J. Organomet. Chem.* **1995**, *486*, 177.
[24] J. A. Fernandes, R. A. Sá Ferreira, M. Pillinger, L. D. Carlos, J. Jepsen, A. Hazell, P. Ribeiro-Claro, I. S. Gonçalves, *J. Lumin.,* in press.
[25] J.-C. G. Bünzli, in *Lanthanide Probes in Life, Chemical, and Earth Sciences* (Eds.: J.-C. G. Bünzli, G. R. Choppin), Elsevier, Amsterdam, **1989**, p. 219.
[26] [26a] L. D. Carlos, R. A. Sá Ferreira, V. de Zea Bermudez, C. Molina, L. A. Bueno, S. J. L. Ribeiro, *Phys. Rev. B* **1999**, *60*, 10042. [26b] O. L. Malta, H. J. Batista, L. D. Carlos, *Chem. Phys.* **2002**, *282*, 21.
[27] [27a] O. L. Malta, M. A. Couto dos Santos, L. C. Thompson, N. K. Ito, *J. Lumin.* **1996**, *69*, 77. [27b] O. L. Malta, H. F. Brito, J. F. S. Menezes, F. R. Gonçalves e Silva, S. Alves Jr., F. S. Farias Jr., A. V. M. de Andrade, *J. Lumin.* **1997**, *75*, 255.
[28] M. H. V. Werts, R. T. F. Jukes, J. W. Verhoeven, *Phys. Chem. Chem. Phys.* **2002**, *4*, 1542.
[29] M. F. Hazenkamp, G. Blasse, *Chem. Mater.* **1990**, *2*, 105.
[30] C. W. Struck, W. H. Fonger, *Understanding Luminescence Spectra and Efficiency Using Wp and Related Functions*, Springer-Verlag, Berlin, **1978**.
[31] C. de Mello Donegá, S. J. L. Ribeiro, R. R. Gonçalves, G. Blasse, *J. Phys. Chem. Solids* **1996**, *11*, 1727.
[32] G. Blasse, N. Sabbatini, *Mater. Chem. Phys.* **1987**, *16*, 237.
[33] J.-C. G. Bünzli, P. Froidevaux, J. M. Harrowfield, *Inorg. Chem.* **1993**, *32*, 3306.
[34] R. Longo, F. R. Gonçalves e Silva, O. L. Malta, *Chem. Phys. Lett.* **2000**, *328*, 67.
[35] O. L. Malta, personal communication.
[36] R. G. Charles, A. Perrotto, *J. Inorg. Nucl. Chem.* **1964**, *26*, 373.
[37] R. Colton, I. B. Tomkins, *Aust. J. Chem.* **1965**, *18*, 447.
[38] M. J. Frisch, G. W. Trucks, H. B. Schlegel, G. E. Scuseria, M. A. Robb, J. R. Cheeseman, V. G. Zakrzewski, J. A. Montgomery, R. E. Stratmann, J. C. Burant, S. Dapprich, J. M. Millam, A. D. Daniels, K. N. Kudin, M. C. Strain, O. Farkas, J. Tomasi, V. Barone, M. Cossi, R. Cammi, B. Mennucci, C. Pomelli, C. Adamo, S. Clifford, J. Ochterski, G. A. Petersson, P. Y. Ayala, Q. Cui, K. Morokuma, D. K. Malick, A. D. Rabuck, K. Raghavachari, J. B. Foresman, J. Cioslowski, J. V. Ortiz, B. B. Stefanov, G. Liu, A. Liashenko, P. Piskorz, I. Komaromi, R. Gomperts, R. L. Martin, D. J. Fox, T. Keith, M. A. Al-Laham, C. Y. Peng, A. Nanayakkara, C. Gonzalez, M. Challacombe, P. M. W. Gill, B. G. Johnson, W. Chen, M. W. Wong, J. L. Andres, M. Head-Gordon, E. S. Replogle, J. A. Pople, GAUSSIAN 98 (Revision A.1), Gaussian, Inc., Pittsburgh, PA, **1998**.
[39] L. F. Pacios, P. A. Christiansen, *J. Chem. Phys.* **1985**, *82*, 2664.
[40] W. Stevens, H. Basch, J. Krauss, *J. Chem. Phys.* **1984**, *81*, 6026.
[41] W. J. Stevens, M. Krauss, H. Basch, P. G. Jasien, *Can. J. Chem.* **1992**, *70*, 612.
[42] L. VanMeervelt, A. Froyen, W. D'Olieslager, C. WalrandGorller, I. Drisque, G. S. D. King, S. Maes, A. T. H. Lenstra, *Bull. Soc. Chim. Bel.* **1996**, *105*, 377.

Received March 9, 2004
Early View Article
Published Online July 29, 2004

